J Solid State Electrochem (2012) 16:2861–2866
DOI 10.1007/s10008-012-1714-7

ORIGINAL PAPER

Electrochemical synthesis of nano-cobalt hexacyanoferrate at a sol–gel-coated electrode templated with β-cyclodextrin

Mario Berrettoni · Marco Giorgetti · James A. Cox · David Ranganathan · Paolo Conti · Silvia Zamponi

Received: 20 January 2012 / Revised: 29 February 2012 / Accepted: 4 March 2012 / Published online: 16 March 2012

Abstract The paper describes the time-dependent evolution of the electrochemical deposition of cobalt hexacyanoferrate (CoHCFe) on graphite foil electrode modified with electrochemically formed sol–gel film doped with β-cyclodextrin to impart porosity. With short-time electrodeposition, cyclic voltammetry (CV) shows a single redox couple typical of nano-sized clusters of CoHCFe, while at longer deposition times the CV's shape evolves to the classical form of a bulk compound in which there are present two redox couples. The electrode modified with β-cyclodextrin (CD) included in the sol–gel film has an active surface that corresponds to pores created by CD stacks normal to the surface. Hence, the electrochemical formation of CoHCFe starts in these conductive pores; only at long deposition times do the clusters overlap to form moieties with the voltammetric characteristics of bulk CoHCFe.

Keywords Cobalt hexacyanoferrates · Electrochemical deposition · Modified electrode · Silica-coated electrode · Nano-sized materials

M. Berrettoni (✉) · M. Giorgetti
Dipartimento di Chimica Fisica ed Inorganica,
Università di Bologna e Unità di Ricerca INSTM di Bologna,
Viale del Risorgimento 4,
40136 Bologna, Italy
e-mail: mario.berrettoni@unibo.it

J. A. Cox · D. Ranganathan
Department of Chemistry and Biochemistry, Miami University,
Oxford, OH 45056, USA

D. Ranganathan · P. Conti · S. Zamponi
Scuola di Scienze e Tecnologie, Università di Camerino,
Via S. Agostino 1,
62032 Camerino, Italy

Introduction

Molecular imprinting is a process that utilizes the molecular recognition phenomena between a template molecule and the monomers employed in the polymerization of a rigid macroporous polymer, to create a unique network of microporous cavities within the polymer matrix [1]. The development of these materials has become one of the most promising fields in modern materials chemistry for its extensive applications in separation, absorption, catalysis, sensor, and in biological and medical diagnostics [2]. Cyclodextrins (CDs), cyclic oligosaccharides consisting of six to eight D-glucose units linked by a-1,4-glucose bonds, have been employed as structure-directing agents to obtain silica sol–gel materials with the 0.7-nm core of the CD providing a pore structure [3]. In this regard, stacking of CD units into a structure perpendicular to an electrode has been reported [4]. Moreover, the stacking of CD units can also lead to formation of a worm-like structure with greater diameter pores [5].

From the synthetic point of view, one of the important subjects in the study of nanoparticles is to prepare well-dispersed nanoparticles with homogeneous size in a controlled manner. Recent studies suggested that the controlling growth of metal coordination polymers under spatial confinement could be a good methodology to synthesize nanoscale materials with a wide range of chemical compositions [6]. Controlling the growth of materials at the submicrometer scale is of central importance in the emerging field of nanotechnology. Although considerable effort has been dedicated to the controlled synthesis of metals, oxides, sulfides, and ceramic materials with nanoscale dimension, little attention has focused to date on supramolecular compounds

such as coordination polymers. In this regard, transition metal hexacyanometalates, with the general composition $A_i^{m+}\left[B(CN)_6\right]^{n-}$, consist of a large homologous series of molecule-based magnetic materials generally obtained by simple coprecipitation processes [7]. They exhibit unique magnetic behavior depending on their constituents and ratios of transition metal ions, and have played important roles in the field of molecular magnets. Cobalt hexacyanoferrate (CoHCFe), which belongs to the transition metal hexacyanoferrate family, with the generic formula $Co^{m+}[Fe(CN)_6]^{n-}$, is of interest from both fundamental and practical perspectives [8]. Both cobalt and iron have two common oxidation states (II, III) leading to a multitude of compound stoichiometries and redox reactions.

Recently, our group reported on the preparation of cobalt hexacyanoferrate nanoparticles obtained by solution synthesis showing electrochemical behavior dependent on the cluster size [9]. In the present study, control of the cluster size by electrochemical formation of CoHCFe is examined as a mean of controlling the cluster size and distribution. In this regard, the size and shape control of nanoparticles is acknowledged as important to a wide range of catalytic application [10].

Experimental

Reagents

Tetraethylorthosilicate (TEOS) at more than 99 % purity, β-cyclodextrin (β-CD) hydrate, lithium perchlorate, ferrocene (98 %), potassium chloride, and cobalt chloride hexahydrate were obtained from Aldrich (Milwaukee, WI). The anhydrous 2-propanol (99.5 %) was obtained from Alfa Aesar (Ward Hill, MA), $K_3Fe(CN)_6$ from J. T. Baker (Phillipsburg, NJ). All the chemicals were reagent grade and were used as received. All solutions were prepared with house-distilled water that was further purified with a Barnstead NANO pure system.

Experimental procedures

Electrochemical experiments were carried out with the CH Instruments (Austin, TX) models 400, 660B, or 800 electrochemical workstations. The working electrode was a graphite foil (GFE). All potentials were measured versus an Ag|AgCl, 3 M KCl reference electrode from Bioanalytical Systems (West Lafayette, IN) unless noted. Platinum gauze was used as counter electrode.

Sol–gel films were electroplated onto graphite foil electrode. Electroplating conditions are according to Cox and coworkers [3, 4], as adapted from Shacham et al. [11–13]. Briefly, the solution from which the films were plated was the following mixture: 11.25 ml anhydrous 2-propanol that was saturated with CD (ca. 10 mM in the final solution), 0.165 g $LiClO_4$, 3 μL H_2O, and 3.75 ml tetraethylorthosilicate. The base electrode was immersed in this solution for 30 min, after which a potential of +2.0 V vs. a platinum quasi-reference electrode was applied for 30 min in stirred solution. During the potential application, the electrode was withdrawn from the plating solution at 500 μm min^{-1}. Electrodes were air dried at least overnight before using for further studies. For electrochemical measurements using the sol–gel electrodes, each coated electrode was cut to have a geometrical area of up to 0.60 cm^2.

Preparation of CoHCF nanorods

The formation of CoHCFe nanorods in the channels of β-CD-templated TEOS electrode was obtained by potentiostatic and potentiodynamic techniques. The typical deposition solution consists of 30 mL 0.1 M KCl and 0.25 mL 0.02 M $CoCl_2$. The β-CD-templated TEOS electrode was immersed into the electroplating solution for 5 min, by stirring the solution, then 0.25 mL of 0.02 M $K_3Fe(CN)_6$ was added and the electrodeposition was started immediately. Under potentiostatic conditions the electrode was kept at +0.0 V, for 60 s or 150 s. Potentiodynamic method involves cycling of the electrode from 0.9 to 0.0 V, at a scan rate of 50 mV s^{-1}. Before electrochemical experiments, all solutions were degassed for 10 min with a stream of pure nitrogen.

Results and discussion

Electrochemically formed CoHCFe on graphite foil modified electrode (GFME) was achieved under potentiostatic and potentiodynamic conditions. The potentiodynamic deposition consists of 100 cycles at 50 mV s^{-1} in the range 0.9–0.0 V vs Ag/AgCl reference electrode; in Fig. 1 is reported the CV for the electrode prepared, as above described, in KCl 0.1 M supporting electrolyte solution while the inset shows the dynamic growth of the CoHCFe film.

The cyclic voltammogram shows the typical shape of CoHCFe prepared by chemical synthesis or by electrodeposition of GC without any added template on the surface, showing two reduction waves: A at 0.7 V and B at 0.45 V. As usual the redox features can be ascribed to the reduction of Fe^{III} to Fe^{II}, peak A, and to the reduction of Co^{III} to Co^{II}, peak B [14, 15]. A close inspection of the growing cycles shows an evolution of the CV morphology in which the first cycles show only the peak B. In Fig. 2 are compared the second cycle and the last one.

The evolving CV morphology can be fixed by using a potentiostatic deposition technique with different deposition

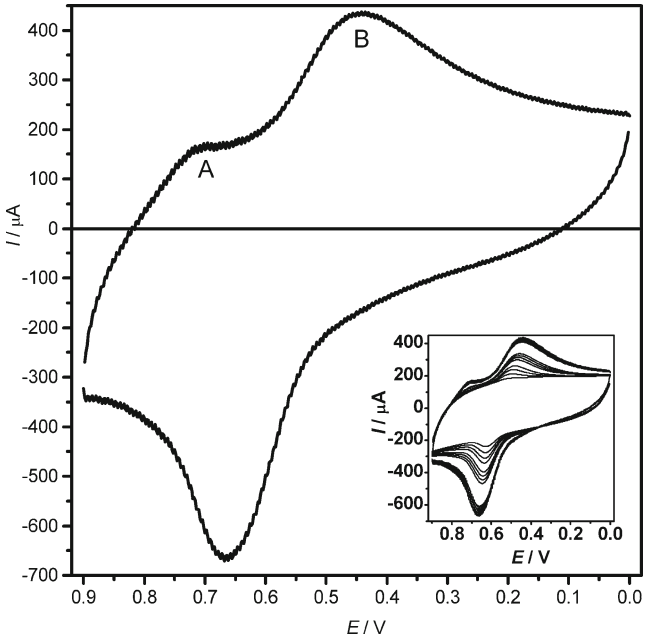

Fig. 1 Cyclic voltammetry of electrochemically formed CoHCFe at GFME electrode in KCl 0.1 M, 50 mVs^{-1}. In the *inset* the CVs during the growing process

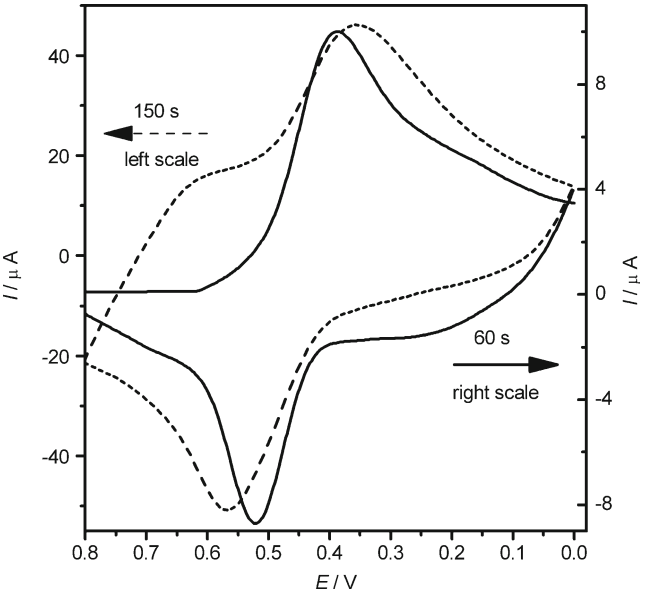

Fig. 3 Cyclic voltammetry of electrochemically formed, potentiostatic mode, CoHCFe at GFME electrode in KCl 0.1 M, 50 mVs^{-1}. *Solid line*: deposition time 60 s, *dashed line*: deposition time 150 s

times. Figure 3 shows the CV for potentiostatic deposition at 0.0 V for 60 and 150 s.

The CVs are plotted after the subtraction of the background current recorded in the solution containing only the supporting electrolyte. To verify the influence of the β-CD-templating agent, the CV obtained under the same conditions of Fig. 3 are reported in Fig. 4 by using bare graphite foil electrode. In this case, the CV obtained at 60 s of deposition is very similar to that obtained at 150 s. Figures 5 and 6 show the SEM images recorded on the electrodes used in Fig. 3.

The formation of CoHCFe is well confirmed by the EDX analysis in the spot mode, Fig. 7, where the contemporary presence of Co and Fe is evident. Figure 8 shows the IR spectra recorded in ATR mode.

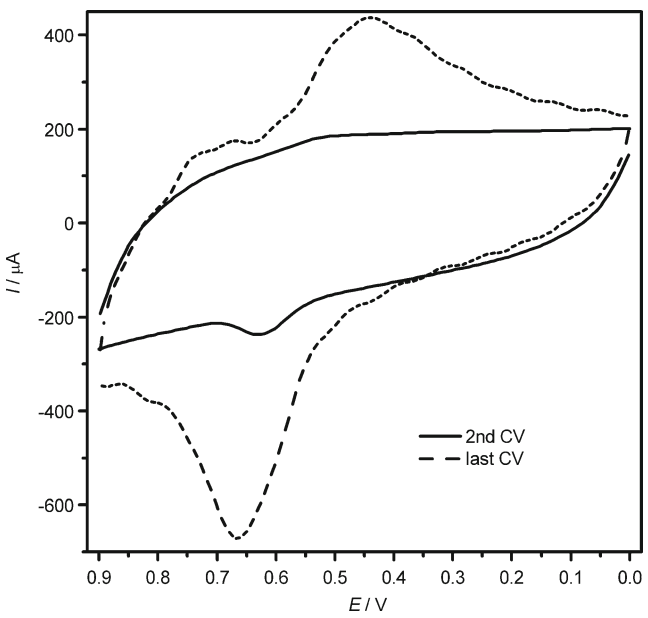

Fig. 2 Comparison of the second cycle (*solid line*) and the last one (*dashed line*) in the growing process

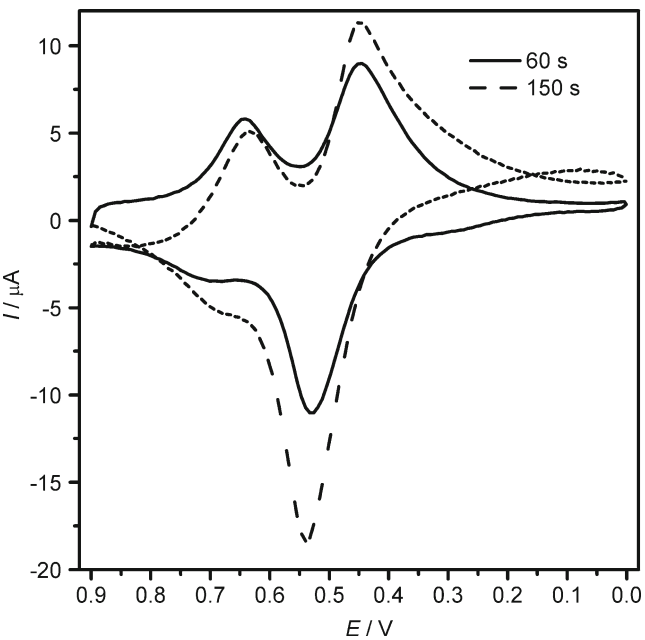

Fig. 4 Cyclic voltammetry of electrochemically formed, potentiostatic mode, CoHCFe at GFE electrode in KCl 0.1 M, 50 mVs^{-1}. *Solid line*: deposition time 60 s, *dashed line*: deposition time 150 s

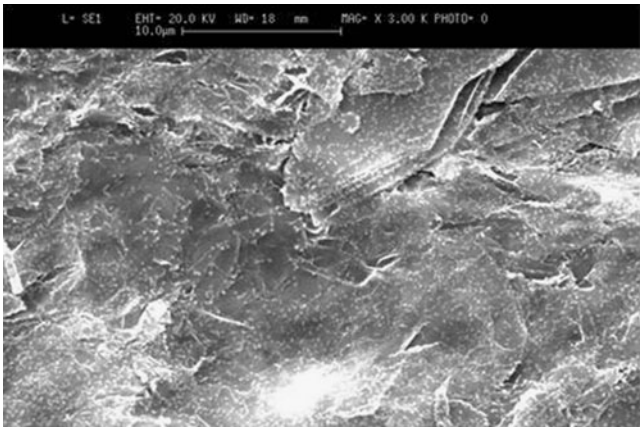

Fig. 5 SEM image of GFME covered with electrochemically formed CoHCFe; deposition time, 60 s

Discussion

The use of β-CD imprinting was based on the hypothesis that its inclusion in the silica film provides a conducting system with controlled pore diameters. The pores define the unique electrochemically active portion of the electrode surface. The electrochemical deposition of CoHCF [16] on this electrode surface becomes dependent on the pores geometry, i.e., diameter and texture. Actually, the electrochemical growth starts in the correspondence of the pores leading to a formation of nano structures. This is well confirmed by the CV recorded at short-time deposition under potentiostatic conditions, or in the first cycles under potentiodynamic mode that show morphology very similar to the one obtained in the nano size CoHCFe [9]. For longer time deposition and higher number of cycles, the CV's morphology evolves towards that obtained on a classic powder or thick film of CoHCFe [9].

The β-CD used in this work has an inner diameter of about 7.5 Å. Considering also this nominal value as the

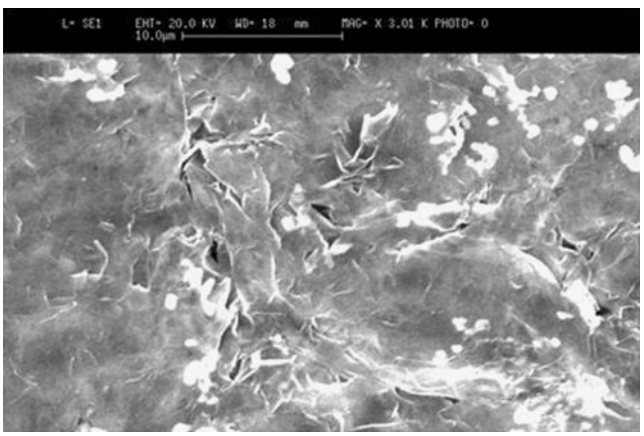

Fig. 6 SEM image of GFME covered with electrochemically formed CoHCFe; deposition time, 150 s

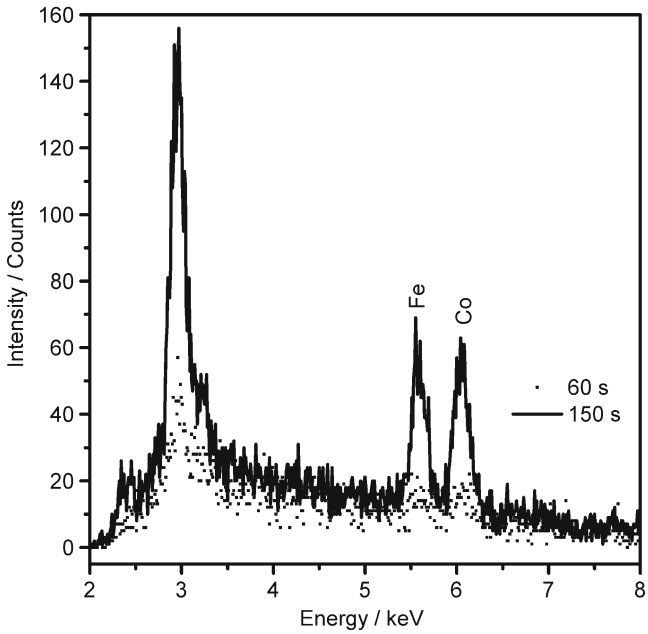

Fig. 7 EDX analysis of GFME covered with electrochemically formed CoHCFe; deposition time 60 s (*dotted line*) and deposition time 150 s (*solid line*)

inner diameter of the channels in the film, which thickness is about 230 nm [4], it is impossible to electroform inside them CoHCFe since the size of the unity cell is very close to 10 Å (see [8] and citations therein). We can hypothesize that the templating process is not due to a single CD unit but to a random cluster, worm-like arrangements [5], of several CD units leading to a formation of islands with a wide range of

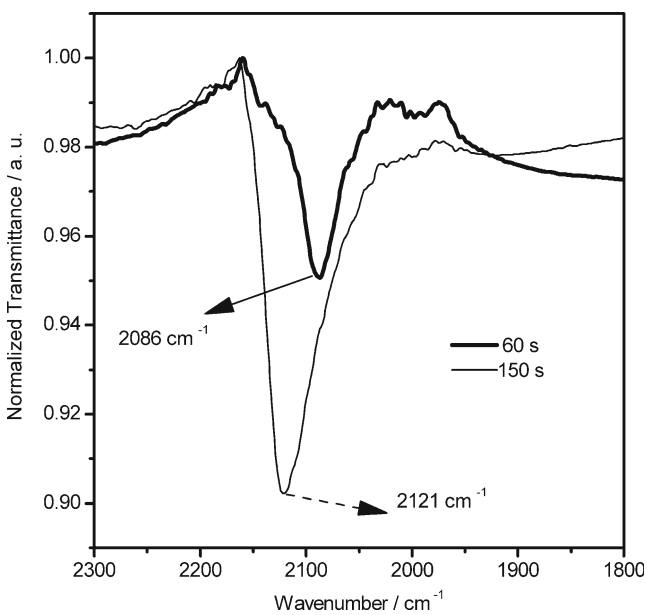

Fig. 8 IR analysis in ATR mode of GFME covered with electrochemically formed CoHCFe; deposition time 60 s (*thick line*) and deposition time 150 s (*thin line*)

inner dimensions. This process allows the electroformation of CoHCFe in the conductive islands having an inner medium diameter greater than 10 Å. The distribution of suitable islands is macroscopically uniform on the electrode surface as can be inferred from Fig. 5. An alternative pictorial way to explain the electrodeposition process is to consider the islands with the suitable inner diameter as nucleation center. Taking into account this electrode morphology, the electrochemical formation of CoHCFe starts into the suitable islands and fulfills them up to the surface where appears as nanoscale spot. The cyclic voltammograms under short-time deposition in potentiostatic mode or in the first cycles, under potentiodynamic mode, show the characteristic morphology of nanoscale compounds [9]. The amount of CoHCFe increases as the deposition time or the number of cycles increase resulting in a spread out of the nano-sized spot to overlap each other. The SEM image in Fig. 6 shows clearly bigger aggregates of CoHCFe. Conversely, the cyclic voltammograms evolve to the typical morphology of the bulk CoHCFe [9]. The formation of CoHCFe is also demonstrated by the results of the EDX, Fig. 7, analyses recorded on the whole area in Fig. 5 and in the spot mode in Fig. 6 show a different amount of the electroformed compound as well as by the IR spectra, Fig. 8, that shows the typical band of the CN stretching in the CoHCFe [15].

Figure 9 reports a possible scheme of the electrochemical grow of CoHCFe at GFME.

A deeper inspection of the cyclic voltammetric features confirms that from the electrochemical point of view the different size is obtained a different deposition time. In the compound CoHCFe, the redox processes can involve both

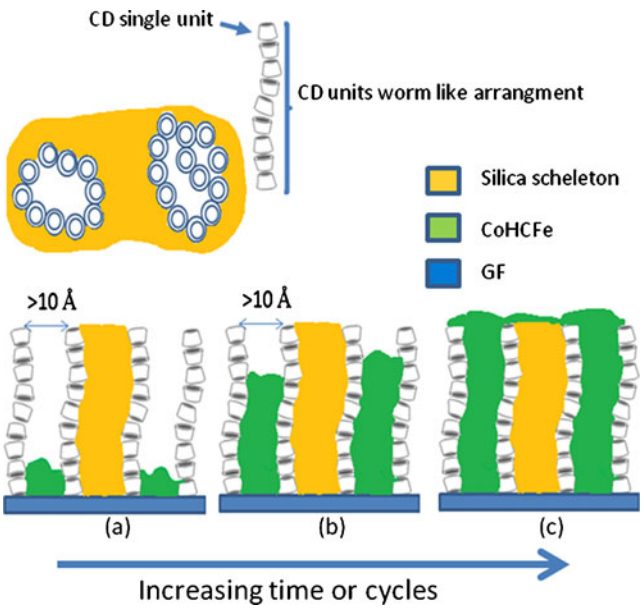

Fig. 9 Probable scheme of CoHCFe electrodeposition on GFME. *a* and *b* nano-size electrochemical behavior; *c* bulk behavior

iron and cobalt center in accord with the following reaction scheme

$$K(CoFe)^{V}(CN)_6 + K^+ + e \rightleftarrows K_2(CoFe)^{IV}(CN)_6 \quad (1)$$

regardless the metal that undergoes to the redox reaction. Actually, both metals can be reduced in the same cycle. The reaction (1) was elucidated by many authors ([7] and references therein) resulting in the attribution of the peak at 0.7 V to the redox couple Fe^{III}/Fe^{II} and the peak at 0.4 V to the couple Co^{III}/Co^{II}. In this class of compounds, the Fe^{III} center is always electrochemically active, while the redox process related to the couple Co^{III}/Co^{II} becomes allowed only for compounds crystallized in the so called insoluble form. For the CoHCFe electroformed, nano-sized like, the external surface plays a key role in the electrochemical process due the fact that the boundary surface can be considered rich in defects resulting in the higher concentration of Co^{III} with respect to Fe^{III}; this condition can lead to a CV that shows only one redox couple at potential attributed to the reduction of Co^{III}. When the aggregate grows, the contribution from the bulk becomes important and hence the CV presents the expected redox features attributed to both metal centers. This findings are confirmed also by IR spectra in which at short-time deposition only the band relative to Fe^{II}–CN–Co^{II} at 2,086 cm^{-1} is present while at higher deposition time the spectra show a convolution of different band contribution due to a mix of chains containing both Fe^{II}, Fe^{III}, and Co^{II}, Co^{III} species. The above statements need to be confirmed by the kinetic study of the redox process. Usually, in this kind of compounds in the bulk form, where the electrochemical process is described by reaction (1), the dependence of the i_p from the scan rate obeys to two different regimes. At high scan rate, the i_p is linear with the square root of the scan rate indicating current controlled by semi-infinite linear diffusion, i.e., the limiting factor is the flux of K^+ ions to the electrode surface. At low scan rate, the i_p becomes linear with the scan rate indicating a surface-confined process in which the limiting factor is the diffusion of K^+ ions inside the structure. Actually, the electrode obtained at longer deposition time behaves in such a way that confirms its higher thickness. In the case of short-time deposition, the i_p is linearly dependent on the square root of the scan rate for all the investigated values confirming that only the surface is involved in the electrochemical redox process.

Conclusions

Graphite foil modified with electrochemically formed sol–gel doped with β-CD can be used to electrodeposit CoHCFe in nano-sized form. The dimension of cluster can be

modulated by varying the deposition time. The nano-sized deposit is confirmed by its electrochemical properties and it was investigated by SEM, EDX, and IR techniques which findings evidence uniquely the formation of CoHCFe. At increasing deposition time, the nano-sized clusters grow up to overlap each other and the electrochemical response becomes typical of the bulk specie. The electrode kinetic study based on the dependence of the i_p vs. scan rate evidences two different diffusion regimes for the nano-sized and bulky compounds. In the bulky compound, the i_p is linear with scan rate at low values and with square root of scan rate at high values, as expected for this class of compounds in which the limiting process is the K^+ ions fed from the solution, at high scan rate, and the diffusion of K^+ ions inside the structure at low scan rate. In the nano-sized specie, the i_p is linear with the square root of scan rate confirming the surface electrochemical process.

References

1. Soares CMF, Zanin GM, de Moraes FF, dos Santos OAA, de Castro HF (2007) J Incl Phenom Macro Chem 57:79–82
2. Wang HC, Li JT, Lin P, Li XB, Bian XB, Wang XM, Li BL (2010) Microporous Mesoporous Mater 134:175–180
3. Ohira A, Ishizaki T, Sakata M, Taniguchi I, Hirayama C, Kunitake M (2000) Colloids Surf A 169:27–33
4. Wandstrat MM, Spendel WU, Pacey GE, Cox JA (2007) Electroanalysis 19:139–143
5. Han BH, Antonietti M (2002) Chem Mater 14:3477–3485
6. Kong Q, Chen X, Yao J, Xue D (2005) Nanotechnology 16:164–168
7. Vaucher S, Fielden J, Li M, Dujardin E, Mann S (2002) Nano Lett 2:225–229
8. de Tacconi NR, Rajeshwar K, Lezna RO (2003) Chem Mater 15:3046–3062
9. Berrettoni M, Giorgetti M, Zamponi S, Conti P, Ranganathan D, Zanotto A, Saladino ML, Caponetti E (2010) J Phys Chem C 114:6401–6407
10. Gilliam RJ, Kirk DW, Thorpe SJ (2011) Electrocatal 2:1–19
11. Shacham R, Avnir D, Mandler D (1999) Adv Mater 11:384–388
12. Shacham R, Mandler D, Avnir D (2004) Chem Eur J 10:1936–1943
13. Shacham R, Anvir D, Mandler D (2004) J Sol–Gel Sci Technol 31:329–334
14. Shi L, Wu T, Wang M, Li D, Zhang Y, Li J (2005) Chin J Chem 23:149–154
15. Lezna RO, Romagnoli R, de Tacconi NR, Rajeshwar K (2002) J Phys Chem B 106:3612–3621
16. Kulesza PJ, Malik MA, Zamponi S, Berrettoni M, Marassi R (1995) J Electroanal Chem 397:287–292